Chelate-free metal ion binding and heat-induced radiolabeling of iron oxide nanoparticles

Eszter Boros,[1,2] Alice M. Bowen,[3] Lee Josephson,[4] Neil Vasdev[2,5] and Jason P. Holland[2,5]*

[1] The Athinoula A. Martinos Center for Biomedical Imaging, 149 13th Street, Suite 2301, Charlestown, Massachusetts, United States of America, 02129

[2] Department of Radiology, Massachusetts General Hospital, Harvard Medical School, 55 Fruit Street, Boston, Massachusetts, United States of America, 02114

[3] Institute of Physical and Theoretical Chemistry, Goethe University Frankfurt, Max-von-Laue-Str. 7, Building N140/Ground Floor, 60438 Frankfurt am Main, Germany

[4] Center for Advanced Molecular Imaging Sciences, Massachusetts General Hospital, Harvard Medical School, 149 13th Street, Charlestown, Massachusetts, United States of America, 02129

[5] Division of Nuclear Medicine and Molecular Imaging, Massachusetts General Hospital, 55 Fruit Street, White 427, Boston, Massachusetts, United States of America, 02114

* Corresponding and Senior Author:

Dr. Jason P. Holland

Tel: +1-(617)-726-6107

Fax: +1-(617)-726-6165

E-mail: holland.jason@mgh.harvard.edu; jasonpholland@gmail.com

Table of Contents

Experimental Methods

General details

All chemicals, unless otherwise stated, were purchased from SigmaAldrich (St. Louis, MO) and were used as received. For labeling reactions, aliquots of a clinical formulated dose of Feraheme (FH; Ferumoxytol inject; 510 mg at 30 mg/mL of Fe; formulated in mannitol [44 mg/mL]; AMAG Pharmaceuticals, Cambridge, MA) was used as received without further puritrcation. For control labeling studies, Molday ION USPIO nanoparticles (size = 70 nm; 10 mg/mL Fe; BioPAL, Worcester, MA) were used as received without further purification. Water (>18.2 MΩ·cm at 25 ºC, Milli-Q, Millipore, Billerica, MA) was purified by passing through a 10 cm column of Chelex resin (Bio-Rad Laboratories, Hercules, CA) at a flow rate <1.0 mL/min to remove common metal ion contaminants. All instruments were calibrated and maintained in accordance with previously reported routine quality-control procedures.[1] Radioactivity was measured by using a Capintec CRC-15R Dose Calibrator (Capintec, Ramsey, NJ) with a calibration factor of 465 for ^{89}Zr, 015 for ^{64}Cu, and 303 for ^{111}In. For accurate quantification of radioactivity, experimental samples were counted for 1 min. on a calibrated Perkin Elmer (Waltham, MA) Automatic Wizard[2] Gamma Counter using a dynamic energy window of 800–1000 keV for ^{89}Zr (909 keV emission), 450–600 keV for ^{64}Cu (511 keV emission), and 150–300 keV for ^{111}In (171 and 245 keV emissions). Appropriate decay correction was employed throughout. Radiolabeling reactions were monitored by using thin-layer chromatography (with silica gel 60 F_{254} on aluminium strips [EMD Chemicals Inc., Darmstadt, Germany] or Whatman 3MM filter paper strips [Whatman International Ltd., Maidstone, United Kingdom]) and analyzed either visually (for Fe nanoparticles = orange) or by using a radio-TLC plate reader (Bioscan System 200 Imaging Scanner coupled to a Bioscan Autochanger 1000 (Bioscan Inc., Washington, DC, using Win-Scan Radio-TLC software version 2.2). Solvent systems included diethylene triamine pentaacetic acid in water (DTPA, 50 mM, pH7), Chelex-treated water, standard saline, and phosphate buffered saline (PBS; pH7.4). Solution pH was measured by using either a calibrated pH meter (Denver Instruments, Arvada, CO) or pH paper strips (colorpHast non-bleeding strips; EMD Chemicals Inc., Gibbstown, NJ). Electronic absorption (UV/vis) spectra were recorded on Evolution 300 UV-vis spectrometer Thermo Scientific) equipped with VISIONpro 4.20 software.

Radionuclides

Zirconium-89 was produced *via* the ^{89}Y$(p,n)^{89}$Zr transmutation reaction on an GE PETtrace (16.5 MeV) cyclotron equipped with a custom-made solid target assembly (BTI Targetry, LLC, Inc., Cary, NC, USA) in accordance with previously reported methods.[2] The ^{89}Zr-oxalate was isolated in high radionuclidic and radiochemical purity (RCP) >99.9%, with an effective specific-activity of 0.470 – 1.195 Ci/μmol. ^{89}Zr-oxalate in 1.0 M oxalic acid was reformulated to produce ^{89}Zr-chloride in 1.0 M HCl(aq.) in accordance with previously reported methods involving extraction onto an activated QMA strong-anion exchange cartridge.[2] Copper-64 dichloride formulated in

1.0 M HCl (effective specific activity ~13.0 Ci/μmol at end of bombardment [EOB]) was purchased from Prof. Jerry Nickles at the University of Wisconsin-Madison, USA. Indium-111 chloride was purchased from Nordion Inc., Vancouver, Canada.

Radiochemistry

Radiolabeling of USPIO nanoparticles with $^{64}Cu^{2+}$ (chloride), $^{111}In^{3+}$ (chloride) or $^{89}Zr^{4+}$ (chloride or oxalate) was accomplished using the same general conditions. Briefly, an aqueous solution of radioactivity (ca. 0.3 – 5.0 mCi; volume approximately 0.1 – 0.7 mL; pH <1.0) in either 1.0 M HCl(aq.) or 1.0 M oxalic acid, was transferred to a metal-free vial and the solution was neutralized by addition of small aliquots of 1.0 M Na_2CO_3(aq.). CAUTION: Acid neutralization with Na_2CO_3(aq.) generates CO_2(g) and care should be taken to avoid loss of radioactivity from the dissolution vessel. The pH of the stock radioactivity solution was adjusted to the range 7.1 – 9.0 (typically pH7.9 – 8.3). During the optimization of radiolabeling conditions, aliquots of ~130 μCi of activity were used for each reaction. Aliquots of radioactivity at the desired pH were transferred to 1.0 mL metal-free Reacti-Vial™ glass vials (Thermo Fisher Scientific Inc., Rockford, IL) and solutions were diluted to 380 μL with Chelex-treated water to which was added 20 μL of the stock solution of nanoparticle (e.g. formulated Feraheme [FH]; stock Fe concentration = 30 mg/mL; 0.6 mg/reaction; 1.826 nmol of particles; 10.73 μmol total Fe) giving a total reaction volume of 400 μL. A small magnetic stir bar was added to each vial and the reaction vessels were sealed. Reactions were allowed to proceed for between 15 min – 2 h (typically 1 h), at temperatures ranging from room temperature (RT; 20 °C) to 120 °C. At the end of the specified reaction time, the reactions were allowed to cool to RT before being quenched by the addition of a 50 μL solution of desferrioxamine B mesylate (DFO; 10 mM; pH7.0), DTPA (10 mM; pH7.5), EDTA (10 mM; pH7.0), or a DTPA/EDTA mixture (10 mM / each chelate; pH7.0). Quenching reactions were allowed to proceed at RT for between 30 min to 2 h. Radiolabeled nanoparticles were purified by using size-exclusion chromatography (SEC; e.g. PD-10 column eluted with fractions of sterile saline) or spin-column centrifugation (4 mL total volume, <30 kDa particle retention, Amicon Ultra-4, Millipore, Billerica, MA; washed with 4×3 mL sterile saline; 4000 rpm; 10 – 12 min/each wash). The radiochemical purity (RCP) and radiochemical conversion yields of the isolated and formulated radiolabeled nanoparticles were measured by using both radio-TLC and analytical SEC. Overall radiochemical yields (RCYs) were measured for the formulated samples using a dose calibrator (values were corrected for radioactive decay). In typical radio-TLC experiments, ^{89}Zr-FH and ^{89}Zr-DFO were retained on silica gel plates and remained at the baseline (R_f = 0.0), whereas $^{89}Zr^{4+}$(aq.) ions coordinated as ^{89}Zr-DTPA eluted with the solvent front (R_f = 1.0).

Stability studies: ligand challenge experiments

The radiochemical stability of radiolabeled FH was evaluated by performing ligand challenge experiments. Briefly, samples of radiolabeled nanoparticles (e.g. ^{89}Zr-FH; 200 μCi; ~50 μL) were added to 450 μL solutions of sterile saline, DFO (10 mM; pH7.0), DTPA (50 mM; pH7.5); EDTA (10 mM; pH7.0) or a DTPA/EDTA mixture (10 mM / each chelate; pH7.0) and reactions

were incubated at 37 °C for 72 h. Aliquots (15 µL) were removed at 0, 24, 48 and 72 h and analysis of radiochemical stability was performed by using analytical size-exclusion chromatography (SEC; PD-10 columns eluted with 40 × 0.2 mL fractions of sterile saline). Activity eluted in the first 1.8 mL was associated with the high-molecular weight (>30 kDa) fraction whereas activity eluted in the fractions >2.0 mL was associated with small-molecules (typically ^{64}Cu, ^{111}In or ^{89}Zr metal ions coordinated by the chelating agents DFO, DTPA or EDTA) derived from radiochemical decomposition under the ligand challenge conditions. All experiments were performed in triplicate.

Stability studies: plasma stability studies

The radiochemical stability of radiolabeled FH was also evaluated by performing plasma stability studies. Samples of radiolabeled nanoparticles (e.g. ^{89}Zr-FH; 200 µCi; ~50 µL) were incubated in either rat or human plasma (450 µL) for 72 h at 37 °C. Samples were analyzed by using analytical SEC (PD-10 columns eluted with 40 × 0.2 mL fractions of sterile saline). This experiment was used to assess changes in radiochemical purity and small-molecule release from decomposition of radiolabeled FH in the presence of plasma. All experiments were performed in triplicate.

Non-radioactive metal ion labeling reactions

To facilitate a more detailed chemical analysis of metal ion binding to FH, reactions were performed using non-radioactive metal ion salts. Metal ion chloride salts evaluated for their potential to associate to FH under chelate-free, heat-induced labeling conditions include the *p*-block ion In^{3+}, first row *d*-block transition metal ions Mn^{2+}, Co^{2+}, Ni^{2+}, Cu^{2+} and Zn^{2+}, second row *d*-block transition metal ion Zr^{4+}, and *f*-block lanthanide ions Eu^{3+} and Tb^{3+}. Non-radioactive labeling reactions were conducted under the same conditions used in the radioactive studies (*vide supra*). Temperatures were varied between RT and 100 °C and reactions were incubated for 1 h before quenching with 50 µL solutions of DFO (10 mM; pH7.0) or DTPA/EDTA (10 mM / each chelate; pH7.0). Metal ion stock solutions were prepared with concentrations ranging from 0.16 – 0.55 mM. In the radiochemical reactions, given the typical range of specific activities (e.g. ^{89}Zr specific activity = 470 – 1195 Ci/mmol),[2] 1.0 mCi of activity contains approximately 0.8 – 2.2 nmol of Zr ions. Convention chemical analysis of such small metal ion concentration was impractical. Therefore, in evaluating metal ion binding to FH the total amount of metal ion used in each reaction was between 13.2 – 82.1 nmol, representing between 10 – 100 fold excess of metal ion compared to the radiochemical experiments. In addition to non-radioactive measurements used to assess the absolute binding yield of various metal ions to FH under different temperatures and conditions, we also performed competition studies to evaluate the role of metal ion binding in the presence of other competing metal ions. In metal ion competition binding assays, reaction mixtures containing ~50 nmol of each of the 9 metal ions listed above were prepared and reacted with FH at different temperatures from RT – 100 °C. After incubating for 1 h, samples were cooled, quenched with a 50 µL aliquot of a solution containing a mixture

of DFO/DTPA/EDTA (10 mM / each chelate; pH7.0) and the nanoparticle fractions were isolated by using size-exclusion chromatography (PD-10 column; collecting the first 1.8 mL fraction; eluted in sterile saline). Samples were stored at RT prior to further chemical analysis by electronic absorption spectroscopy, T2 relaxometry, electron spin resonance spectroscopy, dynamic light scattering and induction-coupled plasma-mass spectrometry (*vide infra*). Further, serial dilution studies using varying initial concentrations of $ZrCl_4$ were used to evaluate the maximum Zr^{4+} ion loading capacity of FH. All labeling reactions and appropriate analyses were performed in triplicate.

T2 relaxometry

FH nanoparticles are known to affect the T2 spin-spin proton relaxation time of water. T2 relaxation time measurements were carried out at 0.47 T at 40 °C (Bruker NMR Minispec, Billerica, MA) using solutions with a total Fe content of 5.0 μg/mL. T2 relaxation times were obtained for isolated FH samples labeled with different metal ions, as well as appropriate control samples of FH. All measurements were performed in triplicate in accordance with previously reported methods,[3] and data were expressed as the mean T2 relaxation time (t(T2) / ms) ± one standard deviation (S.D.).

Dynamic light scattering

Particle size distribution was measured by dynamic light scattering (DLS) using a Malvern Zetasizer Nano-ZS (Malvern Instruments Inc., Westborough, MA). Prior to DLS sample preparation, stock sample concentrations were measured by using electronic absorption spectroscopy – absorbance calibration based on the total Fe content FH samples in water at 350 nm gave a measured molar absorption coefficient, ε(350 nm; Fe-total) = 1810 ± 17 mol^{-1} dm^3 cm^{-1}. Then DLS samples containing a total of 5 μg/mL of Fe in sterile saline were prepared and measured in accordance with the manufacturer's recommendations. All experiments were performed in triplicate and individual DLS data sets were taken as the average of 18 separate scans. Particle size data are reported as the range and mean particle radius (r / nm) ± one standard deviation (S.D. / nm).

Electron Magnetic Resonance (EMR) spectroscopy

All nanoparticles were made up to a concentration of 1 mg/mL in a solution of 20% v/v ethylene glycol in water. MR spectra were recorded on a Bruker E500 continuous wave X-band (9.5 GHz) spectrometer fitted with a Bruker continuous flow cryostat. Spectra were recorded at cryogenic temperatures (5 – 200 K) using liquid helium.

Induction-coupled plasma-mass spectrometry (ICP-MS)

Metal ion concentrations were determined using an Agilent 7500a ICP-MS system. All samples were diluted with 0.1% Triton X-100 in 5% nitric acid containing 20 ppb of Lu (as internal standard). The ratio of the main isotope of the metal ion analyzed to Lu (174.97) was used to quantify the metal ion concentration. Linear calibration curves generated from standardized stock

solutions containing known concentrations (from 0.1 – 200 ppb) of metal ions ^{55}Mn, ^{59}Co, ^{60}Ni, ^{63}Cu, ^{66}Zn, ^{90}Zr, ^{115}In, ^{153}Eu and ^{159}Tb were used to quantify metal ion concentration in experimental samples. Samples were measured in triplicate and reported metal ion concentrations are presented as the mean ± one S.D.

Animal husbandy

All animal experiments were conducted in compliance with Institutional Animal Care and Use Committee (IACUC) guidelines and the *Guide for the Care and Use of Laboratory Animals*. Female, wild-type B6C3F1/J mice (6 – 8 weeks old) were obtained from Jackson Laboratory (Bar Harbor, ME). Mice were provided with food and water *ad libitum* and were allowed to acclimatize for 1 week prior to conducting PET/CT and biodistribution experiments.

Small-animal PET/CT imaging

PET/CT imaging experiments were conducted on a dedicated small-animal PET/CT scanner (eXplore Vista-CT, Sedecal, Algete, Spain) equipped with VISTA-CT version 4.11 software. In separate studies (*n*=3), mice were administered formulations of ^{89}Zr-FH (185 – 195 μCi, ~0.20 – 0.21 mg Fe, ~10 mg/kg total Fe dose, specific activity of 0.915 mCi/mg Fe, in 200 μL sterile saline for injection) *via* intravenous (i.v.) tail-vein injection. Approximately 5 minutes prior to recording PET images, mice were anesthetized by inhalation of 3–4% isoflurane (Baxter Healthcare, Deerfield, IL)/oxygen gas mixture and placed on the scanner bed in the prone position. Anesthesia was maintained with 1-2% isoflurane/oxygen gas mixture (flow rate ~5 L/min). Co-registered PET/CT images were recorded at various time-points between 0 – 120 h post-injection (*n*≥3 mice/time point; *n*=5 mice imaged in total). List-mode data were acquired for between 10 and 20 min. per scan using a γ-ray energy window of 250–700 keV. For all static images, scan time was adjusted to ensure ~15 million coincident events were recorded in each acquisition. Data were processed by 3-dimensional Fourier re-binning (3D-FORE), and images were reconstructed using 2-demensional ordered-subset expectation maximum (2D-OSEM) algorithm. Image data were normalized to correct for non-uniformity of response of the PET, dead-time count losses, positron branching ratio, and physical decay to the time of injection, but no attenuation, scatter, or partial-volume averaging correction was applied. An empirically determined system calibration factor (in units of Bq/cps) combined with the decay corrected administered activity and the animal weight were used to parameterize image activity in terms of the standardized uptake value (SUV). Manually drawn 2-dimensional regions-of-interest (ROIs) or 3-dimensional volumes-of-interest (VOIs) were used to determine the maximum and mean SUV radiotracer uptake in various tissues. CT images were recorded using an X-ray current of 300 μA, 360 projections, and an image size of 63.8 mm × 63.8 mm × 46.0 mm. Data were acquired using the Vista CT 4.11 Build 701 software, and reconstructed images were analyzed by using ASIPro VM^{TM} software (Concorde Microsystems) and VivoQuant® 1.23 (InviCRO, LLC, Boston, MA).

Inflammation model

Mouse models of inflammation were developed in accordance with our previous studies[4, 5] by subcutaneous (s.c.) injection of turpentine oil (30 µL, neat) on the right hind limb of female B6C3F1/J mice. Inflammation developed rapidly and mice were subjected to radiotracer administration and temporal PET/CT imaging 16 – 24 h post-administration of turpentine.

Biodistribution studies

Biodistribution studies were conducted to evaluate the uptake of ^{89}Zr-FH in immunocompetent B6C3F1/J mice bearing a subcutaneous inflammation model. Mice were administering ^{89}Zr-FH (15–20 µCi, 16–22 µg of Fe, ~1.0 mg/kg in total Fe dose, in 200 µL sterile saline for injection) *via* i.v. tail-vein injection (*t*=0 h). Animals (*n*=5/per group) were euthanized by CO_2(g) asphyxiation at 1, 4, 24, 48, 72 and 120 h post-radiotracer administration injection and 16 tissues were removed, rinsed in water, dried in air for 5 min., weighed and counted on a calibrated gamma-counter for accumulation of ^{89}Zr-radioactivity. The mass of ^{89}Zr-FH formulation injected into each animal was measured and used to determine the total number of counts (counts per minute, [c.p.m.]) by comparison to a standard syringe of known activity and mass drawn at the same time as the injected doses. Count data were background- and decay-corrected and the tissue uptake measured in units of percentage injected dose per gram (%ID/g) for each sample was calculated by normalization to the total amount of activity injected. Whole-body excretion data in mice (*n*=5) we collected between 0 – 120 h p.i. of ^{89}Zr-FH using a dose calibrator.

Data analysis and statistics

Data and statistical analyses were performed using GraphPad Prism 5.01 (GraphPad Software, Inc., La Jolla, CA) and Microsoft Excel spreadsheets. Biodistribution data were analyzed by using the unpaired, two-tailed Student's *t*-test. Differences at the 95% confidence level (*P*<0.05) were considered to be statistically significant.

Table S1. ICP-MS data of measured specific metal ion binding yields *versus* temperature

	Percentage specific metal ion binding yield / %					
Metal ion	20 °C	40 °C	50 °C	60 °C	80 °C	100 °C
^{90}Zr^{4+}	0.2 ± 0.1	72.4 ± 2.1	81.8 ± 0.8	78.2 ± 2.7	80.5 ± 6.0	83.9 ± 1.0
^{159}Tb^{3+}	0.0 ± 0.1	20.1 ± 1.2	24.0 ± 1.1	23.6 ± 0.1	35.9 ± 2.6	40.3 ± 1.1
^{153}Eu^{3+}	0.3 ± 0.5	27.6 ± 1.9	33.2 ± 1.6	31.1 ± 0.2	39.4 ± 5.0	40.7 ± 1.4
^{115}In^{3+}	0.0 ± 0.0	9.0 ± 0.7	11.3 ± 0.9	10.9 ± 0.6	14.9 ± 2.4	14.1 ± 0.9
^{63}Cu^{2+}	0.5 ± 1.1	23.4 ± 0.1	24.6 ± 0.2	25.9 ± 1.3	29.7 ± 2.0	29.4 ± 0.9
^{60}Co^{2+}	0.1 ± 0.1	28.5 ± 2.6	33.1 ± 1.1	28.8 ± 0.2	35.0 ± 4.1	34.2 ± 1.1
^{59}Ni^{2+}	1.0 ± 0.9	22.6 ± 8.8	24.3 ± 8.0	23.4 ± 8.8	27.1 ± 5.0	24.8 ± 8.0
^{55}Mn^{2+}	40.5 ± 1.4	32.6 ± 1.2	35.9 ± 1.7	40.3 ± 0.9	47.7 ± 6.7	43.3 ± 1.3
^{66}Zn^{2+}	16.9 ± 23.8	53.0 ± 19.6	53.8 ± 19.0	49.1 ± 16.0	59.8 ± 5.2	60.6 ± 10.1

Figure S1. Temperature-dependent X-band ESR spectra of Zr-FH nanoparticles.
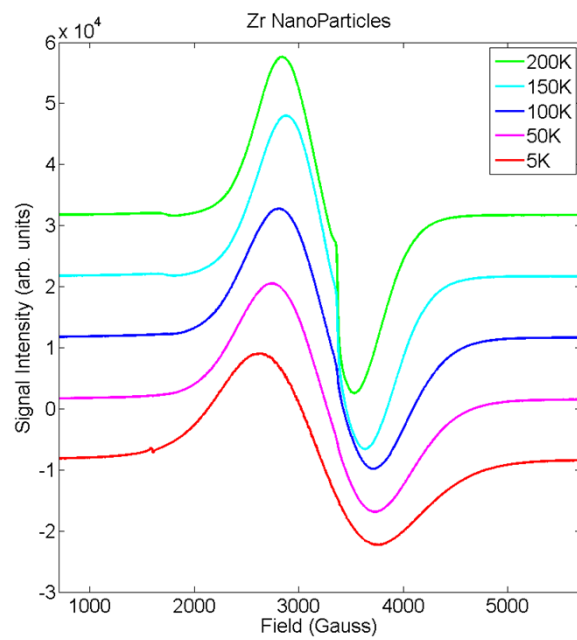
Figure S2. Temperature-dependent X-band ESR spectra of Cu-FH nanoparticles.
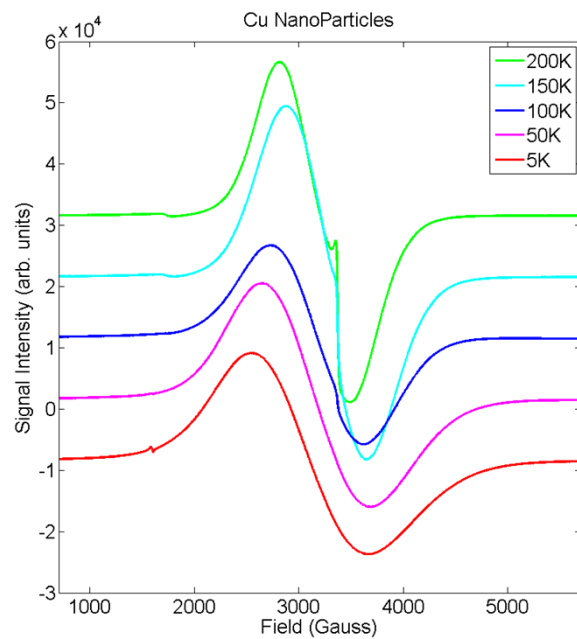
Figure S3. Temperature-dependent X-band ESR spectra of In-FH nanoparticles.
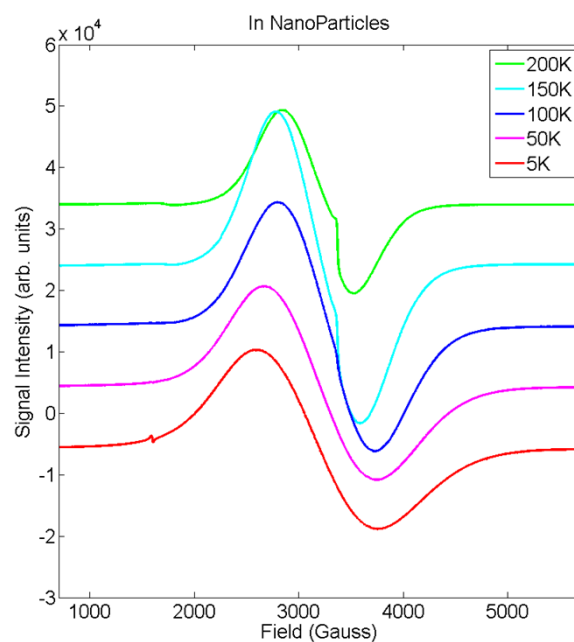
References

1.   P. Zanzonico, *J. Nucl. Med.*, 2009, **49**, 1114-1131.
2.   J. P. Holland, Y. Sheh and J. S. Lewis, *Nucl. Med. Biol.*, 2009, **36**, 729-739.
3.   J. M. Perez, L. Josephson, T. O'Loughlin, D. Hogemann and R. Weissleder, *Nat Biotech*, 2002, **20**, 816-820.
4.   J. P. Holland, M. J. Evans, S. L. Rice, J. Wongvipat, C. L. Sawyers and J. S. Lewis, *Nature Med*, 2012, **18**, 1586-1591.
5.   M. J. Evans, J. P. Holland, S. L. Rice, M. G. Doran, S. M. Cheal, C. Campos, S. D. Carlin, I. K. Mellinghoff, C. L. Sawyers and J. S. Lewis, *J. Nucl. Med.*, 2013, **54**, 90-95.